Geophysical Research Letters

RESEARCH LETTER
10.1029/2018GL080188

The Influence of Competing Hydroclimate Processes on Stable Isotope Ratios in Tropical Rainfall

B. L. Konecky[1,2], D. C. Noone[3], and K. M. Cobb[4]

[1]Department of Earth and Planetary Sciences, Washington University, St. Louis, Missouri, USA, [2]Cooperative Institute for Research in Environmental Sciences, University of Colorado Boulder, Boulder, Colorado, USA, [3]College of Earth, Ocean, and Atmospheric Sciences, Oregon State University, Corvallis, Oregon, USA, [4]School of Earth and Atmospheric Sciences, Georgia Institute of Technology, Atlanta, Georgia, USA

Key Points:
- We present a new conceptual framework and statistical model for the oxygen isotopic composition of precipitation at tropical stations
- Cloud type is leading influence where stratiform rain is abundant; moisture transport plays key role along tropical rain belt perimeters
- $\delta^{18}O_P$ and Precip are both water cycle integrators, but $\delta^{18}O_P$ is a more reliable proxy for large-scale hydrological processes than Precip

Supporting Information:
- Supporting Information S1
- Table S1

Correspondence to:
B. L. Konecky,
bkonecky@wustl.edu

Citation:
Konecky, B. L., Noone, D. C., & Cobb, K. M. (2019). The influence of competing hydroclimate processes on stable isotope ratios in tropical rainfall. *Geophysical Research Letters*, *46*, 1622–1633. https://doi.org/10.1029/2018GL080188

Received 24 AUG 2018
Accepted 28 DEC 2018
Accepted article online 10 JAN 2019
Published online 4 FEB 2019

Abstract In tropical paleoclimate studies, paleo-precipitation is often reconstructed from proxies via the "amount effect," that is, the empirical inverse relationship between local precipitation amount (P) and the oxygen isotopic composition of precipitation ($\delta^{18}O_P$). However, recent research has illustrated numerous microphysical and dynamical controls on $\delta^{18}O_P$ that do not necessarily covary with P, complicating the reconstruction of circulation features like the Intertropical Convergence Zone. Here we introduce a new conceptual and statistical model for $\delta^{18}O_P$ that better captures the physical foundations for $\delta^{18}O_P$ as a tracer of hydrological balance. We find that bulk precipitation microphysics and cloud type exert comparable influences on $\delta^{18}O_P$. Moisture transport plays an important secondary role in regions of deep atmospheric convection such as the Intertropical Convergence Zone and Indo-Pacific Warm Pool. Our findings help reconcile conflicting interpretations of Intertropical Convergence Zone excursions, and provide a firm physical grounding for more nuanced, accurate interpretations of past hydroclimate using water isotope proxies.

Plain Language Summary The oxygen isotopic composition of tropical precipitation is a powerful tool for "fingerprinting" the history of evaporation, condensation, and transport that water was subjected to in the atmosphere before it reached the ground as precipitation. For this reason, the oxygen isotopic composition of precipitation is commonly employed as a water cycle tracer, both in modern-day contexts and in geologic archives. Translating oxygen isotope ratios into metrics of circulation and climate is not always straightforward, however, due to the range of processes that can affect precipitation. Here we introduce a novel conceptual and statistical framework for interpreting oxygen isotope ratios in tropical precipitation by deconvolving its multiple competing influences. We find that the relative importance of each factor varies geographically. Moisture source is particularly important around the Indo-Pacific Warm Pool, while cloud type exerts strong influence in regions where stratiform clouds are abundant. These results help to reconcile conflicting interpretations of how the Intertropical Convergence Zone and other key features of tropical circulation respond to climate forcings, which are critical questions for past climate reconstructions as well as future climate projections.

1. Introduction

The oxygen and hydrogen isotopic composition of precipitation and water vapor ($\delta^{18}O_P$, δD_P, $\delta^{18}O_v$, δD_v; collectively referred to as "water isotopes") are sensitive tracers of the tropical water cycle at multiple scales, from raindrop-level physical processes to large-scale features of atmospheric circulation (Conroy et al., 2016; Dansgaard, 1964; Galewsky et al., 2016; Kurita, 2013; Martin et al., 2018; Moerman et al., 2013; Worden et al., 2007). The isotopic composition of meteoric water is well preserved in terrestrial paleoclimate archives (e.g., ice cores, speleothems, lake sediments), and for most of the tropics, such archives are the primary source of paleoclimate information (PAGES Hydro2k Consortium, 2017). However, global syntheses of paleoclimate data have fallen short of reconstructing paleo-hydroclimatic processes because the interpretation of such proxy records can be complex, due in part to the wide range of processes affecting $\delta^{18}O_P$ and δD_P (Konecky et al., 2018; PAGES Hydro2k Consortium, 2017). The environmental signals contained within $\delta^{18}O_P$ and δD_P are further obscured when detected and transformed within a proxy system (Evans et al., 2013). Even as improvements in proxy system models enable reconstruction of paleo-$\delta^{18}O_P$ and paleo-δD_P with higher and higher fidelity (Dee et al., 2015), translation of

these reconstructions into metrics of a changing water cycle requires decoding the environmental signals contained in $\delta^{18}O_P$ and δD_P.

In paleoclimate studies, tropical $\delta^{18}O_P$ is often interpreted to reflect local precipitation amount (hereafter P) via the "amount effect," that is, the empirical correlation between high monthly P and low monthly $\delta^{18}O_P$ observed at many tropical stations (Dansgaard, 1964). Following this correlation, increased or reduced paleo-precipitation is inferred from lower or higher paleo-$\delta^{18}O_P$ (or δD_P) values, respectively (Schefuß et al., 2005; Wang, 2001; Wang et al., 2017). In some cases, the qualitative inference of wetter versus drier conditions is reasonably supported by independent evidence from other moisture-sensitive proxies (e.g., Schefuß et al., 2005) or modern-day measurements (e.g., Carolin et al., 2013). However, in other cases, independent evidence either contradicts the amount effect—for example, suggesting aridity during periods of low $\delta^{18}O_P$ or δD_P (Konecky et al., 2011, 2016; Wicaksono et al., 2017)—or does not exist at all, such as in some karst settings where speleothem $\delta^{13}C$ or trace element ratios are not viable.

Unrealistic conclusions about the climate system can arise when $\delta^{18}O_P$ and δD_P is assumed to directly reflect local P. For example, several recent studies have utilized proxy-derived inferences of the mean position of the Intertropical Convergence Zone (ITCZ) under past climate states to assess how various climate forcings impact cross-equatorial fluxes of heat and energy; this question is critical for future climate projections (Seidel et al., 2008; Seidel & Randel, 2007). Heat and energy fluxes are strongly correlated to the precipitation-defined ITCZ position, that is, the latitude of the centroid or maximum of tropical zonal mean P, P_{cent}, and P_{max}, respectively (Donohoe et al., 2013; McGee et al., 2014; Roberts et al., 2017). Under the assumption that paleo-$\delta^{18}O_P$ and paleo-δD_P represent local P, P_{cent} or P_{max} could be interpreted to have shifted as far south as 8.5°S during the last glacial period (Ayliffe et al., 2013) and as far north as 20°N during the early Holocene (Fleitmann et al., 2007), excursions of nearly −10° and more than +15°, respectively, relative to modern P_{cent} (McGee et al., 2014). Such excursions far exceed the average ~1° shift predicted by climate models under glacial forcings (Donohoe et al., 2013; McGee et al., 2014) or the 2.5–7° shift over the open ocean reconstructed by non-water isotope proxy data (Reimi & Marcantonio, 2016). Additionally, such excursions are often not supported by co-located or adjacent proxy records for vegetation, surface erosion, and other proxies for P or P-E (Dubois et al., 2014; Konecky et al., 2016; Niedermeyer et al., 2014; Wicaksono et al., 2017). Do models and nonisotopic proxy data underestimate the excursions of the mean position of the ITCZ in response to climate forcings? Or do tropical water isotope proxy records reflect climatic processes that do *not* covary with local P?

Seminal work on the amount effect attributed the correlation between monthly $\delta^{18}O_P$ and P to bulk precipitation microphysical processes (Figure 1), such as increased local humidity during precipitation that limits raindrop re-evaporation and diffusional isotope exchange, and increasing Rayleigh removal of heavy isotopologues as precipitating clouds cool (Dansgaard, 1964; Rozanski et al., 1993). In recent decades, observational and modeling studies have demonstrated multiple facets of atmospheric circulation, moisture trajectories, and cloud type that also exert strong influences on $\delta^{18}O_P$ but are distinct from previous explanations of bulk precipitation microphysics. Circulation drives $\delta^{18}O_P$ through the convergence of water vapor from isotopically distinct moisture sources (Moore et al., 2014), by altering the residence time of water in the atmosphere (Aggarwal et al., 2012), and via variations of large-scale moisture transport into the tropics (Joussaume et al., 1984; Jouzel et al., 1987; Noone & Simmonds, 2002). Alternatively, the specific type of clouds that produce rain—that is, whether isolated convective clouds or deep, horizontally extensive stratiform clouds typically associated with tropical mesoscale convective systems—may also drive $\delta^{18}O_P$, although it is unclear which of many possible mechanisms explains this phenomenon (Aggarwal et al., 2016; Kurita, 2013; Kurita et al., 2011; Risi et al., 2012).

A major shortcoming of many explanations of tropical $\delta^{18}O_P$ is that their influence is most often quantified via a simple linear regression of $\delta^{18}O_P$ against the predictor in question (Aggarwal et al., 2012, 2016; Dansgaard, 1964; Rozanski, 2005). Such an approach is problematic because in nature, predictor variables are often correlated with each other, causing overestimation or underestimation of R^2 depending on the choice, ordering, and interdependence of predictors or the existence of omitted variables. For example, the strong correlation between $\delta^{18}O_P$ and stratiform rain (Aggarwal et al., 2016) may be biased because P itself also tends to increase with higher stratiform rain fraction (Schumacher et al., 2004; Schumacher & Houze, 2003a; 2003b), such that the roles of moisture convergence and microphysical processes like rain re-evaporation (which also increase with P) remain hidden variables in the regression.

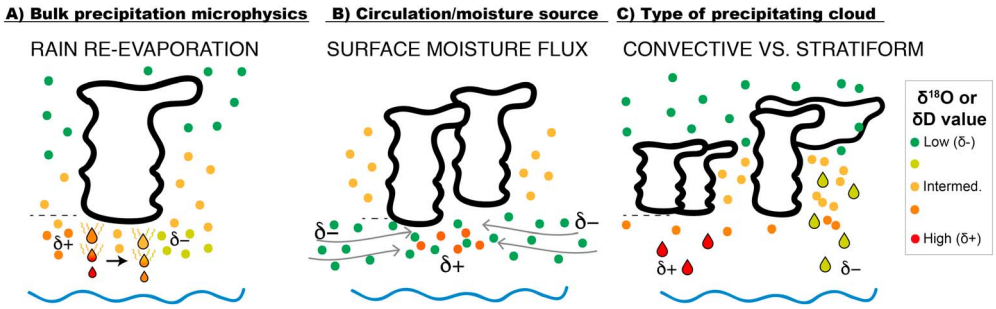

Figure 1. Illustration of fractionating processes in the tropical atmosphere that drive changes in the δD and $\delta^{18}O$ of precipitation and water vapor. The cartoon depicts idealized clouds over the ocean and illustrates three categories of fractionating processes known to influence tropical $\delta^{18}O_P$, including the vertical and temporal evolution of isotope ratios in vapor (circles) and rain (teardrops). (a) Bulk precipitation microphysical processes averaged over many clouds in a region; such processes include the re-evaporation and equilibration of raindrops (shown here), condensation rates, detrainment rates, ice/liquid fraction, and nucleation processes. (b) Moisture transport conditions tied to the large- or regional-scale circulation, encapsulating the direction and magnitude of surface moisture fluxes (shown here), as well as transport characteristics and divergence/convergence. (c) Cloud type, that is, differences between (left) convective and (right) tropical stratiform clouds, including their vertical structure, detrainment/entrainment levels, degree and elevation at which precipitation is formed or re-evaporated, and vertical profiles of latent heating in the troposphere. Note that all three of these categories also influence P itself, as moisture is condensed via microphysical processes (a) during moisture convergence (b) at a level and rate determined by cloud type (c); therefore, each category can be assumed to vary in a manner that could change the correlation between $\delta^{18}O_P$ and P.

Predictor correlation and hidden variables may explain why at most stations, the P-$\delta^{18}O_P$ correlation is very weak, with >80% of variance unexplained (Figure 2a), and also why the amount effect correlation emerges only when ≤daily rainfall has been aggregated to the scale of several days to weeks (Conroy et al., 2016; Moerman et al., 2013). Clearly, a physically and theoretically robust interpretive framework for $\delta^{18}O_P$ is needed that includes, but is not limited to, processes that can produce negative correlations with P. In this study, we present such a framework.

2. Approach

2.1. Conceptual Approach

In this section we outline our conceptual framework for $\delta^{18}O_P$. The problem with local P as a predictor of $\delta^{18}O_P$ is that P, as measured at rainfall stations, integrates a suite of isotopically fractionating processes within the water cycle. In a vertical sense, precipitation at the surface (P_{surf}) occurs when condensation of cloud moisture exceeds the amount of subcloud rain evaporation (RE):

$$P_{surf} = \int(\text{condensation} - \text{RE}) \tag{1}$$

where the amount of P_{surf} is the vertical integral of the difference between condensation and rain evaporation at every below-cloud atmospheric layer. Condensation and RE are microphysical processes occurring within and near clouds, and are dependent on the vertical structure of clouds, types and distribution of cloud nuclei, humidity below the cloud base, various aspects of convective activity, and other characteristics. Hence, P at a given location is ultimately dictated by the bulk microphysics of local precipitating clouds. Each microphysical process causes isotopic fractionation, but to different extents.

From a water budget perspective, P at any given location is balanced by evapotranspiration (ET) of moisture from the Earth's surface into the atmosphere, plus atmospheric transport of moisture into or away from the location, such that

$$P = ET + \text{transport} \tag{2}$$

Inherently, P occurs during moisture convergence. Therefore, while P falls locally, the convergence of the moisture that forms P ultimately depends on atmospheric transport from nonlocal sources or from recycled evapotranspired moisture derived locally.

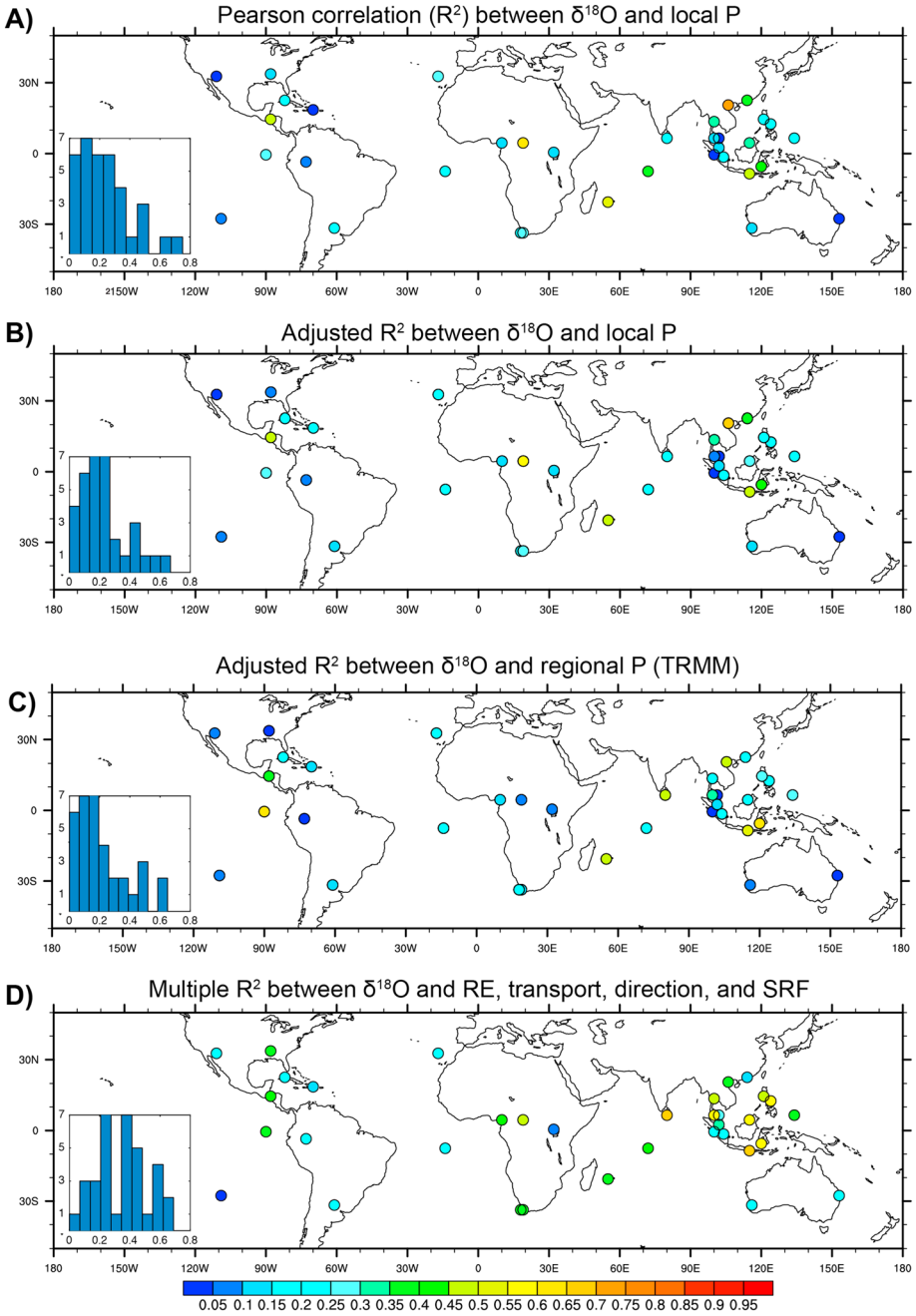

Figure 2. Fraction of variance in monthly average $\delta^{18}O$ explained by regression models. (a) The Pearson R^2 between $\delta^{18}O_P$ and local P measured at GNIP+ stations (the classic amount effect). (b) The R^2 between $\delta^{18}O_P$ and local P when $\delta^{18}O_P$ is modeled against four predictors—P and three randomly generated AR(1) time series—for more robust comparison with a four-predictor multiple regression model. (c) Same as in (b) but using gridbox-scale P from TRMM rather than local station P. (d) Multiple R^2 between $\delta^{18}O_P$ and the final, four-predictor multiple regression model. Inset histograms show the distribution of R^2 across the data set.

Putting equations (1) and (2) together, the water budget of a given geographic location is a balance between local cloud/precipitation microphysics, local ET, and nonlocal atmospheric transport. Therefore, the water isotopic budget depends on the net isotopic composition of condensate after postcondensation evaporation and diffusion ($\delta_{microphys}$), evapotranspiration fluxes to the atmosphere, and converged moisture. Cloud type is fundamentally related to moisture transport and convergence, as increases in tropical stratiform versus convective rain are associated with strengthened upper level circulation (Schumacher et al., 2004). Cloud

type also sets the stage for isotopic fraction during condensation (i.e., a starting point for $\delta_{microphys}$) by determining the level in the atmosphere and the temperature at which condensation forms, as well as ice crystal growth and other factors (Kurita, 2013; Kurita et al., 2011).

In this study, we consider a spatial scale that is too small for local ET to contribute significantly to $\delta^{18}O_P$. The area integrated by a precipitation collection device or a rain gauge at a rainfall station is on the order of meters to tens of meters. Therefore, the majority of converged moisture at a given rain gauge is derived from nonlocal sources rather than from fluxes of ET originating from the same location. The isotopic composition of ET fluxes from a given location does matter for other locations where that moisture is subsequently transported, but that isotopic composition is already incorporated into the $\delta_{transport}$ term.

The resulting theoretical framework considers P and $\delta^{18}O_P$ to be a function of the three remaining categories: bulk precipitation microphysics, cloud type, and transport. Since P and $\delta^{18}O_P$ integrate similar processes within the water cycle, they should behave similarly, and a correlation is to be expected. However, the same physical processes within each category can have different impacts on P versus $\delta^{18}O_P$, for example, two precipitation events of equal magnitude resulting from convergence of moisture from sources with substantially different $\delta^{18}O_P$. Similarly, $\delta_{transport}$ can also be affected by upstream rainout and subsequent reevaporation of falling raindrops, which on its own exerts strong isotopic fractionation but produces negligible P.

$\delta^{18}O_P$ and P at any given station are both water cycle integrators, driven by the convergence of nonlocal moisture, the structure and organization of clouds, and the microphysics of condensation and postcondensation exchanges. However, because $\delta^{18}O_P$ is sensitive to additional processes than P, P and $\delta^{18}O_P$ need not covary. A physically robust model for $\delta^{18}O_P$ must account for the underlying processes that produce precipitation as well as isotopic fractionation: moisture transport, cloud type, and precipitation microphysics.

2.2. Regression Approach

Following the above conceptual approach, we consider monthly tropical $\delta^{18}O_P$ to be a multivariate function of bulk precipitation microphysics, the effects of regional circulation on moisture transport, and cloud type (Figure 1). A multiple linear regression model was constructed to predict $\delta^{18}O_P$ at each station (section 2.3) based on four predictors that represent the three categories in Figure 1:

$$\delta^{18}O_P = \beta_1 \times RE_{frac} + \beta_2 \times MF + \beta_3 \times MTD + \beta_4 \times SRF \quad (3)$$

where β_{1-4} are the coefficients of regression. The variables RE_{frac}, MF, MTD, and SRF correspond to rain reevaporation and sublimation normalized to precipitation, the magnitude of surface moisture fluxes, the direction of surface moisture transport, and stratiform rain fraction, respectively, at each site, following Figure 1 (section 2.3 and supporting information). All variables were selected to have sufficiently high temporal resolution (≤monthly), spatial resolution (≤2.5°), and time coverage (≥10 years), and to maximize temporal overlap among data sets (monthly data from 1998 to 2013).

The variance in $\delta^{18}O_P$ contributed by each of the four variables was partitioned using an R^2 decomposition technique that accounts for collinearity among predictor variables by iteratively calculating different combinations and orderings of predictors (Groemping, 2007). The resulting Relative Importance (RI) of each predictor is defined as the R^2 between the predictor and $\delta^{18}O_P$ averaged over all iterations of the calculation, thereby minimizing competing influence from other predictors (Dobson, 2002). This R^2 decomposition technique has been employed in neuroscience (Freeman et al., 2013; Teicher et al., 2012), population ecology (Treml et al., 2012), and forestry (Castillo-Santiago et al., 2010) studies, but this study is the first application to climate data, to our knowledge.

Our approach differs from previous "isoscapes" of global $\delta^{18}O_P$ based on regressions of available observations against a large number of geographic (e.g., latitude) and climatic (e.g., precipitable water) variables (Terzer et al., 2013), or on spatial interpolation (Bowen & Revenaugh, 2003). The goal of the present study is not to focus solely on statistical relationships in order to predict $\delta^{18}O_P$ where observations are lacking. Rather, the goal is to align a statistical model with a physically based conceptual model, and to use such a model to assess the relative importance of different types of processes on $\delta^{18}O_P$, in order to guide paleoclimate interpretations.

2.3. Selection of Data Sets for Multiple Linear Regression Model

To construct the model, variables were selected to represent the categories represented in Figure 1. Bulk precipitation microphysics (Figure 1a) is represented by the total column re-evaporation and sublimation of precipitation (RE) from the Modern-Era Retrospective Analysis for Research and Applications v.2 (MERRA2) monthly surface flux product (M2TMNXFLX; Bosilovich, 2015; 2017; Rienecker et al., 2008), normalized to precipitation amount at each grid cell, such that $RE_{frac} = RE/(RE + P)$. MERRA2 was selected because of its demonstrated utility for hydrological cycle applications (Bosilovich et al., 2017) and because it is the only reanalysis or satellite product which contains a scientifically validated rain re-evaporation estimate (Bosilovich, 2015). In line with independent observations from Worden et al. (2007), tropical RE_{frac} from MERRA2 generally falls between 20 and 70%, with the lowest values occurring over the eastern Pacific ITCZ region and the highest values occurring along the latitudinal extremes of the rain belt over land, for example, along the southern margins of central Africa where a strong dry season occurs annually (Figure S1). Within the deep tropics, regions that experience heavy year-round precipitation (i.e., the Amazon, Congo, and land areas of the Maritime Continent) tend to experience more moderate RE_{frac} of around 50–60%. Therefore, we take estimates of RE_{frac} from MERRA2 to be satisfactory.

Cloud type (Figure 1c) is represented by the fraction of tropical stratiform versus convective rain (SRF) as observed by the Tropical Rainfall Measuring Mission (TRMM) A23 product from 1998 to 2013 (Schumacher & Houze, 2003a, 2003b). This product classifies tropical stratiform rain as having a radar reflectivity ≥17 dBZ, with weak vertical velocities, low rain rates, and a widespread and homogeneous extent, as is found in tropical stratiform systems that evolve from or are attached to deep convective clouds. Precipitation processes primarily occur in the ice layer above the 0 °C level. Convective rain, on the other hand, is classified as having strong vertical velocities, high rain rates, and isolated and inhomogeneous radar echoes. The SRF product has been vetted elsewhere; details can be found in Schumacher and Houze (2003a) and Schumacher and Houze (2003b).

Circulation (Figure 1b) is represented by two quantities calculated from low-level (850 hPa) assimilated wind and humidity fields from MERRA: the magnitude of horizontal moisture flux (MF) and the transport direction of moisture flux (MTD) at 850 hPa at the grid cell containing each station (SI). Together, MF and MTD capture the two aspects of moisture source, direction and magnitude, that are frequently invoked to explain circulation-driven changes in $\delta^{18}O_P$.

Monthly precipitation amount (P) and precipitation $\delta^{18}O$ ($\delta^{18}O_P$) were analyzed from 35 stations of the Global Network of Isotopes in Precipitation (GNIP; IAEA/WMO, 2018). Stations were screened for quality and data set length by removing stations that did not contain at least two 12-month periods with consecutively reported monthly data. The length of the resulting data set varied by station, ranging from 24 to 607 months. In addition to the GNIP database, six additional stations were included in our analysis: Gunung Buda, Borneo (Moerman et al., 2013), and five other warm pool stations in Bali, Sulawesi, Palau, and Sumatra (Kurita et al., 2009). Collectively, these stations are referred to in the text as "GNIP+." This GNIP+ dataset was previously used to validate the water isotope-enabled Community Earth System Model (Nusbaumer et al., 2017). The δD_P was not analyzed because it was not consistently reported at all stations. All data was placed on a 1° × 1° grid and trimmed to tropical latitudes (35°S–35°N) and from 1998 to 2013, the spatial and temporal extent of the TRMM data set.

2.4. R^2 Decomposition

The relative importance of each of four explanatory variables (RE_{frac}, MF, MTD, SRF) for predicting station $\delta^{18}O_P$ was assessed using a method of R^2 decomposition designed for linear regression models with highly collinear predictors (Dobson, 2002; Groemping, 2007). The method maximizes the largest gain in marginal probability by the addition and placement of each predictor. Linear regression models for station $\delta^{18}O_P$ were calculated iteratively as a sequential sum of squares, with each predictor added one at a time, while varying the number of predictors used in the regression model and their orderings. Varying the number of predictors and their orderings avoids the problem of overestimating or underestimating the importance of one predictor due to its collinearity with another predictor. Otherwise, the ordering of collinear predictors distorts the multiple R^2 of the overall regression model, as well as the individual and partial R^2 between each predictor and the response variable. Calculations were performed with the R package *relaimpo* (Groemping, 2006).

The final metric of "relative importance" of each predictor for $\delta^{18}O_P$ is the average R^2 produced over all iterations of the calculation. This average R^2 is used to assign ranks for each predictor from 1 to 4, where 1 is the most important and 4 is the least. Bootstrapped confidence intervals (90%) on ranks were calculated by sampling the regression model's residuals 1,000 times, and results were used to determine which predictors could be considered first-order within the 90% confidence interval.

To compare R^2 values between a model of $\delta^{18}O_P$ using only one predictor (P) versus a model with multiple predictors, $\delta^{18}O_P$ was modeled as a function of four predictors: P plus three random time series generated to function as predictors 2, 3, and 4 (Figure 2b). Time series were modeled as AR(1) processes with autocorrelation = 0.5 and the number of observations equal to the length of the $\delta^{18}O_P$ time series at each station. The R^2 decomposition then proceeded as above. This approach circumvents the problem that higher R^2 values can result simply from the addition of predictors in a regression model. In order to be consistent with calculations of the amount effect elsewhere in the literature (Dansgaard, 1964; Rozanski et al., 1993), P was not transformed prior to inclusion in the regression models.

3. Results and Discussion

3.1. The $\delta^{18}O_P$ Variance Explained by Multiple Regression Model

At the vast majority of tropical stations, a univariate regression of P against $\delta^{18}O_P$ (i.e., the amount effect) explains only a small fraction of variance in monthly $\delta^{18}O_P$ (median = 22%, range 1–75%; Figure 2b and Table S1). Correlations are especially weak ($R^2 < 0.1$) at seven stations in the western IPWP and the Americas. In other words, the amount effect, when taken at face value (the empirical P versus $\delta^{18}O_P$ correlation), is in fact a poor predictor of monthly $\delta^{18}O_P$ variance. In addition to the nonnormal distribution of P in most locations, the low R^2 likely arises in part from the inherent noisiness of precipitation at any given locality—for example due to orographic variations, rainshadow effects, or localized wind patterns—that obscure the relationship between P and large-scale hydrological conditions at many sites. In this sense, local P is an unreliable proxy for large-scale hydrological processes, whereas $\delta^{18}O_P$ accurately reflects such processes owing to its integrative nature (Moerman et al., 2013).

By contrast, a median of 36% of monthly $\delta^{18}O_P$ variance is explained by the multiple-predictor regression model ("multiple R^2" ranging 4–68%; Figure 2d). The improvement in explained variance is not only due to the inclusion of additional predictors, as the R^2 between P and $\delta^{18}O_P$ remains very similar when $\delta^{18}O_P$ is modeled as a function of P and three randomly generated AR(1) time series ("adjusted R^2," median = 20%, range 1–67%; Figure 2b). The improvement is also not just due to the larger spatial scale integrated by predictor variables in the multiple regression models, that is, some artifact of a "regional amount effect": the adjusted R^2 between P and $\delta^{18}O_P$ is similar or even lower when $\delta^{18}O_P$ is predicted using a more regional metric of P, that is, TRMM precipitation in the 1° grid box containing each GNIP station (median = 16%, range 0–65%; Figure 2c). In the multiple-predictor regression model (Figure 2d), marked improvements are observed in the IPWP and the Americas (Figure 2b versus Figure 2d), and $R^2 < 0.1$ at only two tropical stations. The distribution of R^2 values is strongly skewed toward 0 when only P is considered (skewness = 1.01, an asymmetrical tail toward higher values), but becomes closer to normally distributed when considering the multiple regression model (skewness = 0.26), suggesting particular improvement to stations where correlations between $\delta^{18}O_P$ and P are the weakest. Generally, higher R^2 indicates that bulk microphysical characteristics, cloud type, and circulation processes capture more variance in $\delta^{18}O_P$ than P on its own, even though P itself covaries with each of the predictors. In essence, $\delta^{18}O_P$ is generally more effective than local P at tracing integrated, regional-scale hydrological characteristics.

3.2. Bulk Precipitation Microphysics and Cloud Type Exert Comparable Influence on $\delta^{18}O_P$

Although it has been suggested that SRF is the leading driver of $\delta^{18}O_P$ in the tropics (Aggarwal et al., 2016), RE_{frac} is in fact dominant at a nearly equal number of sites, explaining the most variance in $\delta^{18}O_P$ at 15 stations (compared with 16 where SRF is the dominant factor), and the second-most at an additional 8–9 (Figure 3a). However, while cloud type is not the sole driver of tropical $\delta^{18}O_P$, it is clearly a leading influence in the regions of the tropical rain belt (TRB; defined as the oceanic ITCZ plus the land-based monsoons) where tropical stratiform rain is most abundant (Figure S1; Schumacher & Houze, 2003a), that is, along the oceanic ITCZ, in the IPWP, and in northwestern South America (Figure 3).

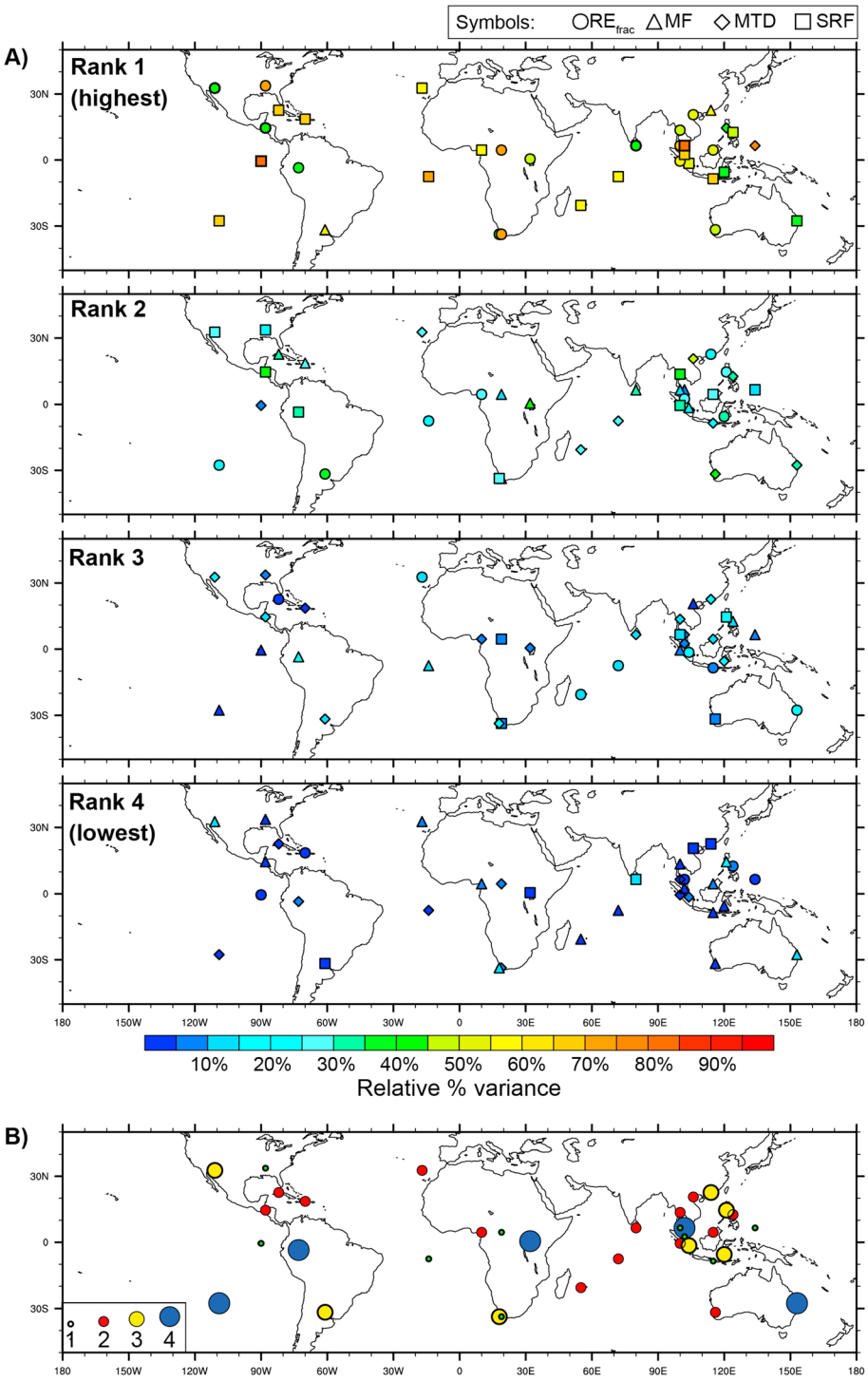

Figure 3. Relative importance of rain evaporation, moisture flux, moisture transport direction, and stratiform rain fraction for monthly average $\delta^{18}O_P$ variance at each station. (a) Relative importances, ranked from the most important predictor (top) to the least important predictor (bottom) at each site. Symbols show which predictor falls into that rank at each station. Shading corresponds to the relative importance of that predictor, that is, the average R^2 after accounting for collinearity of other predictors, relative to the total variance explained by the model at each site ($R^2_{predictor}$/multiple R^2_{model}) (Figure 2b). (b) The number of predictors at each station that can be considered a first-order (rank 1, highest RI) predictor of monthly $\delta^{18}O_P$ within the 90% confidence interval. Size of and color of circle corresponds to the number of predictors.

By contrast, in locations where stratiform rain is not easily sustained, for example outside the TRB and in some land regions within the TRB, RE_{frac} and moisture source play a more dominant role. This is especially apparent in central Africa, which has some of the highest RE_{frac} in the tropics (~0.6) but notably low SRF (Figure S1; Dansgaard, 1964; Rozanski et al., 1993; Schumacher & Houze, 2006), potentially because while precipitation is associated with intense mesoscale convective systems (Jackson et al., 2009), sustained convection is limited by a strong diurnal heating cycle and midlevel intrusions of dry air from the Sahara that limit the development of stratiform rain (Schumacher & Houze, 2006). Therefore, the distribution of stratiform rain in the tropics may itself dictate the importance of cloud type for $\delta^{18}O_P$; this relationship itself could vary in time if the distribution of stratiform rainfall were to change substantially, which could be possible under different land-sea configurations such as in the IPWP during the last glacial period (Konecky et al., 2016).

3.3. Origins of the Regional Amount Effect in the Indo-Pacific Warm Pool

Moisture source has been suggested as an important influence on tropical $\delta^{18}O_P$ (Aggarwal et al., 2016; Griffiths et al., 2013; Kurita, 2013; Kurita et al., 2011; Risi et al., 2012). Indeed, MF and MTD are common secondary influences on $\delta^{18}O_P$ across the tropical rain belt region, particularly along the perimeters of the ITCZ and in the western Indo-Pacific warm pool (Figure 3a). The strong influence of moisture source on tropical $\delta^{18}O_P$ provides a mechanistic origin for the regional amount effect noted in the IPWP (Brienen et al., 2013; Kurita et al., 2009; Moerman et al., 2013; Schumacher et al., 2004; Schumacher & Houze, 2003a, 2003b). The regional amount effect refers to the weak correlation between $\delta^{18}O_P$ and P at the same station, but a stronger correlation with P across a broader region (Aggarwal et al., 2016; Conroy et al., 2016; Kurita et al., 2009; Moerman et al., 2013; Figure 2c). Contrary to the interpretation of the amount effect in these studies, this phenomenon cannot originate from bulk precipitation microphysical processes occurring in local precipitating clouds during monsoon season, because such processes would result in strong, not weak, correlations with local P. Rather, our results suggest that boundary layer $\delta^{18}O_{vapor}$ carries a strong "memory" of previous rainout and mixing of air masses (Galewsky et al., 2016; Noone, 2012), which then influences the resulting $\delta^{18}O_P$ when that moisture that is transported and ultimately converged. Such processes have previously been demonstrated to influence the imprint of precipitation processes on atmospheric water vapor (Galewsky et al., 2016). In other words, both moisture source and cloud type could explain the regional amount effect; these effects can, but need not, accompany changes in local P.

We note that the regression presented here is necessarily oversimplified. Representative variables were chosen because comprehensive observations of important processes such as Rayleigh distillation do not exist. This could explain why more than 50% of the variance in $\delta^{18}O_P$ remains unexplained by our model at nearly all stations. Future investigations with isotope-enabled climate models may clarify the role of such processes relative to the processes investigated here, and may also clarify the stationarity of these relationships on geologic time scales. We also note that, as future data sets become available, the conceptual framework presented here could be revised to better maximize independence between predictor terms while incorporating as many physical processes as possible. Despite these caveats, our approach enables multiple influences on $\delta^{18}O_P$ at a given site to be explicitly examined, which will aid the interpretation of $\delta^{18}O_P$ in terms of modern and past climate.

4. Implications for ITCZ Reconstruction Under Past Climate States

The empirical amount effect reflects the influence of as many hydroclimatic processes as influence P itself, but fails to capture a host of other key influences on $\delta^{18}O_P$ variability. This is because P itself is an unreliable integrator of regional-scale hydrological balance. While many previous investigations have highlighted one specific mechanistic origin of the amount effect, results here show that no single category of fractionating processes (Figure 1) can explain $\delta^{18}O_P$ on its own. At most sites, two or three predictors could be considered first-order when accounting for the 90% bootstrapped confidence interval of each rank (Figure 3b). Thus, the predominance of any single factor can be overemphasized when its collinearity with other important influences are not accounted for, providing at least partial reconciliation of prior controversy that stems from the desire to identify a single ubiquitous cause.

The interpretation of $\delta^{18}O_P$ variability in terms of P alone undervalues the utility of information recorded in $\delta^{18}O_P$ variations, at best, and yields grossly inaccurate hydroclimate interpretations, at worst. Relaxing the assumption that $\delta^{18}O_P$ reflects local P, however, enables more robust and powerful inferences of physical climate processes using paleo-water isotope records. For example, the competing influences of the processes in Figure 1 could explain why proxies for P and P-E versus proxies for $\delta^{18}O_P$ have disagreed on whether the IPWP was wet or dry during last glacial period (Ayliffe et al., 2013; Di Nezio et al., 2016; Dubois et al., 2014; Konecky et al., 2016; Niedermeyer et al., 2014; Wicaksono et al., 2017): at that time, the exposure of the Sunda and Sahul shelves and weakening of the Walker circulation likely drove changes in both moisture sources and cloud type, fundamentally altering the amount effect relationship and producing more isotopically light precipitation during periods of aridity (Konecky et al., 2014, 2016; Wicaksono et al., 2017). In addition, although 10°–20° meridional displacements of the ITCZ mean position during the Last Glacial Maximum and the early Holocene cannot be ruled out, it is more likely that such excursions in $\delta^{18}O_P$ and δD_P reflect a combination of local precipitation microphysics, moisture source, and cloud type.

Revised interpretations of these records reveal the power of water isotope proxies: rather than revealing the latitude P_{cent} or P_{max}, isotopic records appear more sensitive to energetic aspects of the ITCZ that are difficult to infer from other archives, such as the transport of moist static energy (related to surface moisture convergence) and dry static energy (related to the three-dimensional vertical circulation and mixing in the atmosphere; Donohoe et al., 2013; Roberts et al., 2017). As the modern "energy flux equator" is offset from P_{cent} by several degrees of latitude (Roberts et al., 2017), it should not be surprising to observe differences in ITCZ position reconstructions via proxies for $\delta^{18}O_P$ versus proxies for P or P-E. Moreover, because forced changes in cross-equatorial atmospheric heat transport are larger for an energy-defined ITCZ versus a precipitation-defined ITCZ (Roberts et al., 2017), a dense, spatially distributed network of isotopic, P, and P-E proxies would allow multiple aspects of cross-equatorial energy and heat fluxes to be reconstructed side-by-side with precipitation impacts. Paired with continuous collections of $\delta^{18}O_P$ data during the modern satellite era, these reconstructions will enable researchers to disentangle changes in tropical P versus changes in interhemispheric energy balance under twenty-first-century climate forcings—including a projected northward migration of the zonal-mean ITCZ (Schneider et al., 2014), decreased vertical mixing and weakening tropical overturning circulation (Vecchi et al., 2006), and a widening of the TRB (Seidel & Randel, 2007)—as they occur.

Acknowledgments
This research was supported by the National Science Foundation through grants NSF-AGS 1433408 to B. Konecky, NSF-P2C2 1203928, 1203785, and 1464824 to K. Cobb and D. Noone, and NSF AGS-1502806 to D. Noone. The authors wish to thank J. Nusbaumer (NASA-GISS) for the assistance with GNIP data and helpful discussions, C. Schumacher and A. Funk for the assistance with the TRMM SRF product, and four anonymous reviewers for the helpful feedback. In accordance with the AGU data policy, the relevant computer code for this manuscript will be available at time of publication from the corresponding author's Github site: https://github.com/bkonecky/tropical_d18O.

References

Aggarwal, P. K., Alduchov, O. A., Froehlich, K. O., Araguas-Araguas, L. J., Sturchio, N. C., & Kurita, N. (2012). Stable isotopes in global precipitation: A unified interpretation based on atmospheric moisture residence time. *Geophysical Research Letters*, *39*, L11705. https://doi.org/10.1029/2012GL051937

Aggarwal, P. K., Romatschke, U., Araguás Araguás, L., Belachew, D., Longstaffe, F. J., Berg, P., et al. (2016). Proportions of convective and stratiform precipitation revealed in water isotope ratios. *Nature Geoscience*, *9*(8), 624–629. https://doi.org/10.1038/ngeo2739

Ayliffe, L. K., Gagan, M. K., Zhao, J. X., Drysdale, R. N., Hellstrom, J. C., Hantoro, W. S., et al. (2013). Rapid interhemispheric climate links via the Australasian monsoon during the last deglaciation. *Nature Communications*, *4*, 2908. https://doi.org/10.1038/ncomms3908

Bosilovich, M. G. (2015). MERRA-2: Initial evaluation of the climate, edited by R. D. Koster. *Technical Report Series on Global Modeling and Data Assimilation*, *43*.

Bosilovich, M. G., Robertson, F. R., Takacs, L., Molod, A., & Mocko, D. (2017). Atmospheric water balance and variability in the MERRA-2 reanalysis. *Journal of Climate*, *30*(4), 1177–1196. https://doi.org/10.1175/JCLI-D-16-0338.1

Bowen, G., & Revenaugh, J. (2003). Interpolating the isotopic composition of modern meteoric precipitation. *Water Resources Research*, *39*(10), 1299. https://doi.org/10.1029/2003WR002086

Brienen, R. J. W., Hietz, P., Wanek, W., & Gloor, M. (2013). Oxygen isotopes in tree rings record variation in precipitation delta O-18 and amount effects in the south of Mexico. *Journal of Geophysical Research: Biogeosciences*, *118*, 1604–1615. https://doi.org/10.1002/2013JG002304

Carolin, S. A., Cobb, K. M., Adkins, J. F., Clark, B., Conroy, J. L., Lejau, S., et al. (2013). Varied response of Western Pacific hydrology to climate forcings over the last glacial period. *Science*, *340*(6140), 1564–1566. https://doi.org/10.1126/science.1233797

Castillo-Santiago, M. A., Ricker, M., & de Jong, B. H. J. (2010). Estimation of tropical forest structure from SPOT-5 satellite images. *International Journal of Remote Sensing*, *22*(4), 449–476. https://doi.org/10.1177/030913339802200402

Conroy, J. L., Noone, D., Cobb, K. M., Moerman, J. W., & Konecky, B. L. (2016). Paired stable isotopologues in precipitation and vapor: A case study of the amount effect within western tropical Pacific storms. *Journal of Geophysical Research: Atmospheres*, *121*, 3290–3303. https://doi.org/10.1002/2015JD023844

Dansgaard, W. (1964). Stable isotopes in precipitation. *Tellus*, *16*(4), 436–468.

Dee, S., Emile-Geay, J., Evans, M. N., Allam, A., Steig, E. J., & Thompson, D. M. (2015). PRYSM: An open-source framework for PRoxY system modeling, with applications to oxygen-isotope systems. *Journal of Advances in Modeling Earth Systems*, *7*, 1220–1247. https://doi.org/10.1002/2015MS000447

Di Nezio, P. N., Timmermann, A., Tierney, J. E., Jin, F.-F., Otto-Bliesner, B., Rosenbloom, N., et al. (2016). The climate response of the Indo-Pacific warm pool to glacial sea level. *Paleoceanography*, *31*, 866–894. https://doi.org/10.1002/2015PA002890

Dobson, A. J. (2002). *An Introduction to Generalized Linear Models*, (2nd ed.). Bocan Raton, FL: Chapman & Hall/CRC.

Donohoe, A., Marshall, J., Ferreira, D., & Mcgee, D. (2013). The relationship between ITCZ location and cross-equatorial atmospheric heat transport: From the seasonal cycle to the Last Glacial Maximum. *Journal of Climate*, *26*(11), 3597–3618. https://doi.org/10.1175/JCLI-D-12-00467.1

Dubois, N., Oppo, D. W., Galy, V. V., Mohtadi, M., van der Kaars, S., Tierney, J. E., et al. (2014). Indonesian vegetation response to changes in rainfall seasonality over the past 25,000 years. *Nature Geoscience*, *7*(7), 513–517. https://doi.org/10.1038/ngeo2182

Evans, M. N., Tolwinski-Ward, S. E., Thompson, D. M., & Anchukaitis, K. J. (2013). Applications of proxy system modeling in high resolution paleoclimatology. *Quaternary Science Reviews*, *76*, 16–28. https://doi.org/10.1016/j.quascirev.2013.05.024

Fleitmann, D., Burns, S. J., Mangini, A., Mudelsee, M., Kramers, J., Villa, I., et al. (2007). Holocene ITCZ and Indian monsoon dynamics recorded in stalagmites from Oman and Yemen (Socotra). *Quaternary Science Reviews*, *26*(1-2), 170–188. https://doi.org/10.1016/j.quascirev.2006.04.012

Freeman, J., Ziemba, C. M., Heeger, D. J., Simoncelli, E. P., & Movshon, J. A. (2013). A functional and perceptual signature of the second visual area in primates. *Nature Neuroscience*, *16*(7), 974–981. https://doi.org/10.1038/nn.3402

Galewsky, J., Steen Larsen, H. C., Field, R. D., Worden, J., Risi, C., & Schneider, M. (2016). Stable isotopes in atmospheric water vapor and applications to the hydrologic cycle. *Reviews of Geophysics*, *54*, 809–865. https://doi.org/10.1002/2015RG000512

Griffiths, M. L., Drysdale, R. N., Gagan, M. K., Zhao, J.-X., Hellstrom, J. C., Ayliffe, L. K., & Hantoro, W. S. (2013). Abrupt increase in east Indonesian rainfall from flooding of the Sunda shelf ~9500 years ago. *Quaternary Science Reviews*, *74*, 273–279. https://doi.org/10.1016/j.quascirev.2012.07.006

Groemping, U. (2006). Relative importance for linear regression in R: The package relaimpo. *Journal of Statistical Software*, *17*(1). https://www.jstatsoft.org/index.php/jss/article/view/v017i01/v17i01.pdf

Groemping, U. (2007). Estimators of relative importance in linear regression based on variance decomposition. *American Statistician*, *61*(2), 139–147. https://doi.org/10.1198/000313007X188252

IAEA, WMO (2018). Global Network of Isotopes in Precipitation: The GNIP Database. *Accessible at http://www.iaea.orgwater*

Jackson, B., Nicholson, S. E., & Klotter, D. (2009). Mesoscale convective systems over Western equatorial Africa and their relationship to large-scale circulation. *Monthly Weather Review*, *137*(4), 1272–1294. https://doi.org/10.1175/2008MWR2525.1

Joussaume, S., Sadourny, R., & Jouzel, J. (1984). A general circulation model of water isotope cycles in the atmosphere. *Nature*, *311*(5981), 24–29. https://doi.org/10.1038/311024a0

Jouzel, J., Russell, G. L., Suozzo, R. J., Koster, R. D., White, J. W. C., & Broecker, W. S. (1987). Simulations of the HDO and H 218O atmospheric cycles using the NASA GISS general circulation model: The seasonal cycle for present-day conditions. *Journal of Geophysical Research*, *92*, 14739. https://doi.org/10.1029/JD092iD12p14739

Konecky, B., Comas-Bru, L., Dassié, E., DeLong, K., & Partin, J. (2018). Piecing together the big picture on water and climate. *Eos*, *99*. https://doi.org/10.1029/2018EO095283

Konecky, B., Russell, J., & Bijaksana, S. (2016). Glacial aridity in central Indonesia coeval with intensified monsoon circulation. *Earth and Planetary Science Letters*, *437*, 15–24. https://doi.org/10.1016/j.epsl.2015.12.037

Konecky, B., Russell, J., Vuille, M., & Rehfeld, K. (2014). The Indian Ocean zonal mode over the past millennium in observed and modeled precipitation isotopes. *Quaternary Science Reviews*, *103*, 1–18. https://doi.org/10.1016/j.quascirev.2014.08.019

Konecky, B. L., Russell, J. M., Johnson, T. C., Brown, E. T., Berke, M. A., Werne, J. P., & Huang, Y. (2011). Atmospheric circulation patterns during late Pleistocene climate changes at Lake Malawi, Africa. *Earth and Planetary Science Letters*, *312*(3-4), 318–326. https://doi.org/10.1016/j.epsl.2011.10.020

Kurita, N. (2013). Water isotopic variability in response to mesoscale convective system over the tropical ocean. *Journal of Geophysical Research: Atmospheres*, *118*, 10,376–10,390. https://doi.org/10.1002/jgrd.50754

Kurita, N., Ichiyanagi, K., Matsumoto, J., Yamanaka, M. D., & Ohata, T. (2009). The relationship between the isotopic content of precipitation and the precipitation amount in tropical regions. *Journal of Geochemical Exploration*, *102*(3), 113–122. https://doi.org/10.1016/j.gexplo.2009.03.002

Kurita, N., Noone, D., Risi, C., Schmidt, G. A., Yamada, H., & Yoneyama, K. (2011). Intraseasonal isotopic variation associated with the Madden-Julian Oscillation. *Journal of Geophysical Research-Atmospheres*, *116*, D24101. https://doi.org/10.1029/2010JD015209

Martin, N. J., Conroy, J. L., Noone, D., Cobb, K. M., Konecky, B. L., & Rea, S. (2018). Seasonal and ENSO influences on the stable isotopic composition of Galápagos precipitation. *Journal of Geophysical Research: Atmospheres*, *123*, 261–275. https://doi.org/10.1002/2017JD027380

McGee, D., Donohoe, A., Marshall, J., & Ferreira, D. (2014). Changes in ITCZ location and cross-equatorial heat transport at the Last Glacial Maximum, Heinrich Stadial 1, and the mid-Holocene. *Earth and Planetary Science Letters*, *390*, 69–79. https://doi.org/10.1016/j.epsl.2013.12.043

Moerman, J. W., Cobb, K. M., Adkins, J. F., Sodemann, H., Clark, B., & Tuen, A. A. (2013). Diurnal to interannual rainfall $\delta^{18}O$ variations in northern Borneo driven by regional hydrology. *Earth and Planetary Science Letters*, *369-370*, 108–119. https://doi.org/10.1016/j.epsl.2013.03.014

Moore, M., Kuang, Z., & Blossey, P. N. (2014). A moisture budget perspective of the amount effect. *Geophysical Research Letters*, *41*, 1329–1335. https://doi.org/10.1002/2013GL058302

Niedermeyer, E. M., Sessions, A. L., Feakins, S. J., & Mohtadi, M. (2014). Hydroclimate of the western Indo-Pacific warm pool during the past 24,000 years. *Proceedings of the National Academy of Sciences*, *111*(26), 9402–9406. https://doi.org/10.1073/pnas.1323585111

Noone, D. (2012). Pairing measurements of the water vapor isotope ratio with humidity to deduce atmospheric moistening and dehydration in the tropical midtroposphere. *Journal of Climate*, *25*(13), 4476–4494. https://doi.org/10.1175/JCLI-D-11-00582.1

Noone, D., & Simmonds, I. (2002). Associations between $\delta^{18}O$ of water and climate parameters in a simulation of atmospheric circulation for 1979–95. *Journal of Climate*, *15*(22), 3150–3169. https://doi.org/10.1175/1520-0442(2002)015<3150:ABOOWA>2.0.CO;2

Nusbaumer, J., Wong, T. E., Bardeen, C., & Noone, D. (2017). Evaluating hydrological processes in the Community Atmosphere Model Version 5 (CAM5) using stable isotope ratios of water. *Journal of Advances in Modeling Earth Systems*, *9*, 949–977.

PAGES Hydro2k Consortium (2017). Comparing proxy and model estimates of hydroclimate variability and change over the common era. *Climate of the Past*, *13*(12), 1851–1900. https://doi.org/10.5194/cp-13-1851-2017

Reimi, M. A., & Marcantonio, F. (2016). Constraints on the magnitude of the deglacial migration of the ITCZ in the central equatorial Pacific Ocean. *Earth and Planetary Science Letters*, *453*, 1–8. https://doi.org/10.1016/j.epsl.2016.07.058

Rienecker, M. M., Suarez, M. J., Todling, R., Bacmeister, J., Takacs, L., Liu, H.-C., et al. (2008). The GEOS-5 Data Assimilation System-Documentation of versions 5.0.1, 5.1.0, and 5.2.0. edited by M. J. Suarez, Technical Report Series on Global Modeling and Data Assimilation.

Risi, C., Noone, D., Worden, J., Frankenberg, C., Stiller, G., Kiefer, M., et al. (2012). Process-evaluation of tropospheric humidity simulated by general circulation models using water vapor isotopic observations: 2. Using isotopic diagnostics to understand the mid and upper tropospheric moist bias in the tropics and subtropics. *Journal of Geophysical Research-Atmospheres*, *117*, D05304. https://doi.org/10.1029/2011JD016623

Roberts, W. H. G., Valdes, P. J., & Singarayer, J. S. (2017). Can energy fluxes be used to interpret glacial/interglacial precipitation changes in the tropics? *Geophysical Research Letters*, *44*, 6373–6382. https://doi.org/10.1002/2017GL073103

Rozanski, K. (2005). Isotopes in atmospheric moisture. In P. K. Aggarwal, J. R. Gat, & K. Froehlich (Eds.), *Isotopes in the Water Cycle: Past, Present and Future of a Developing Science* (pp. 291–302). The Netherlands: IAEA. https://doi.org/10.1007/1-4020-3023-1_18

Rozanski, K., Araguás Araguás, L., & Gonfiantini, R. (1993). Isotopic patterns in modern global precipitation. In P. K. Swart, K. C. Lohmann, J. Mckenzie, & S. Savin (Eds.), *Climate Change in Continental Isotopic Records*, *Geophysical Monograph Series* (Vol. 78, pp. 1–36). Washington DC: American Geophysical Union.

Schefuß, E., Schouten, S., & Schneider, R. R. (2005). Climatic controls on central African hydrology during the past 20,000 years. *Nature*, *437*(7061), 1003–1006. https://doi.org/10.1038/nature03945

Schneider, T., Bischoff, T., & Haug, G. H. (2014). Migrations and dynamics of the Intertropical Convergence Zone. *Nature*, *513*(7516), 45–53. https://doi.org/10.1038/nature13636

Schumacher, C., & Houze, R. A. (2003a). Stratiform rain in the tropics as seen by the TRMM precipitation radar. *Journal of Climate*, *16*(11), 1739–1756. https://doi.org/10.1175/1520-0442(2003)016<1739:SRITTA>2.0.CO;2

Schumacher, C., & Houze, R. A. (2003b). The TRMM precipitation radar's view of shallow, isolated rain. *Journal of Applied Meteorology*, *42*(10), 1519–1524. https://doi.org/10.1175/1520-0450(2003)042<1519:TTPRVO>2.0.CO;2

Schumacher, C., & Houze, R. A. Jr. (2006). Stratiform precipitation production over sub-Saharan Africa and the tropical East Atlantic as observed by TRMM. *Quarterly Journal of the Royal Meteorological Society*, *132*(620), 2235–2255. https://doi.org/10.1256/qj.05.121

Schumacher, C., Houze, R. A., & Kraucunas, I. (2004). The tropical dynamical response to latent heating estimates derived from the TRMM precipitation radar. *Journal of the Atmospheric Sciences*, *61*(12), 1341–1358. https://doi.org/10.1175/1520-0469(2004)061<1341:TTDRTL>2.0.CO;2

Seidel, D. J., Fu, Q., Randel, W. J., & Reichler, T. J. (2008). Widening of the tropical belt in a changing climate. *Nature Geoscience*, *1*(1), 21–24. https://doi.org/10.1038/ngeo.2007.38

Seidel, D. J., & Randel, W. J. (2007). Recent widening of the tropical belt: Evidence from tropopause observations. *Journal of Geophysical Research*, *112*(D20), D20113. https://doi.org/10.1029/2007JD008861

Teicher, M. H., Anderson, C. M., & Polcari, A. (2012). Childhood maltreatment is associated with reduced volume in the hippocampal subfields CA3, dentate gyrus, and subiculum. *Proceedings of the National Academy of Sciences*, *109*(9), E563–E572. https://doi.org/10.1073/pnas.1115396109

Terzer, S., Wassenaar, L. I., Araguas-Araguas, L. J., & Aggarwal, P. K. (2013). Global isoscapes for delta O-18 and delta H-2 in precipitation: Improved prediction using regionalized climatic regression models. *Hydrology and Earth System Sciences*, *17*(11), 4713–4728. https://doi.org/10.5194/hess-17-4713-2013

Treml, E. A., Roberts, J. J., Chao, Y., Halpin, P. N., Possingham, H. P., & Riginos, C. (2012). Reproductive output and duration of the pelagic larval stage determine seascape-wide connectivity of marine populations. *Integrative and Comparative Biology*, *52*(4), 525–537. https://doi.org/10.1093/icb/ics101

Vecchi, G., Soden, B., Wittenberg, A., Held, I. M., Leetmaa, A., & Harrison, M. J. (2006). Weakening of tropical Pacific atmospheric circulation due to anthropogenic forcing. *Nature*, *441*(7089), 73–76. https://doi.org/10.1038/nature04744

Wang, X., Edwards, R. L., Auler, A. S., Cheng, H., Kong, X., Wang, Y., et al. (2017). Hydroclimate changes across the Amazon lowlands over the past 45,000 years. *Nature*, *541*(7636), 204–207. https://doi.org/10.1038/nature20787

Wang, Y. J. (2001). A high-resolution absolute-dated Late Pleistocene monsoon record from Hulu Cave, China. *Science*, *294*(5550), 2345–2348. https://doi.org/10.1126/science.1064618

Wicaksono, S. A., Russell, J. M., Holbourn, A., & Kuhnt, W. (2017). Hydrological and vegetation shifts in the Wallacean region of central Indonesia since the Last Glacial Maximum. *Quaternary Science Reviews*, *157*, 152–163. https://doi.org/10.1016/j.quascirev.2016.12.006

Worden, J., Noone, D., Bowman, K., & Tropospheric Emission Spectrometer Science Team and Data contributors (2007). Importance of rain evaporation and continental convection in the tropical water cycle. *Nature*, *445*(7127), 528–532. https://doi.org/10.1038/nature05508